

THE PERFORMANCE OF WEAR RESISTANCE AND MECHANICAL PROPERTIES FOR THE TITANIUM NITRIDE

M.Yugandhar¹, V.M.Lakshmaiah²

R. Siva Prasad³, Dr.B.Prabhakar kammar⁴

¹Associate Professor with HOD & Research scholar in -VTU, Department of Mechanical Engineering, Newtons institute of science and technology College, Guntur, AP, India.

²Assistant professor - Department of Mechanical Engineering, Newtons institute of science and technology College, Guntur, AP, India.

³Assistant professor - Department of Mechanical Engineering, Newtons institute of science and Technology College, Guntur, AP, (India)

⁴New Horizon Engineering College –Professor in Mechanical Department

ABSTRACT

Three body abrasion in the present study, TiN–NiMo composites were re milled to particle size of 250–315 µm and used as reinforcements for NiCrBSi alloy by plasma transferred arc hardfacing process. The manufactured hard facing alloy was characterised in terms of microstructure, mechanical properties and abrasive wear resistance. Deposition results indicate good quality thick coating with uniform distribution of hard cermet (TiN–NiMo) particles in the matrix, minimum level of hard particle dissolution and low porosity of the hard facing. Cermet particles remain in initial form and consist of agglomerates (TiN and (Ti,Mo)C grains) embedded into Ni-based matrix. The mechanical properties of the TiN and (Ti,Mo)C phases measured by Nano indentation are very similar exhibiting a narrow distribution. The nano-scratching test reveals excellent bonding between the matrix and cermets in the hard facing. No crack propagation was found in the interface matrix/hard phase region. The abrasive wear results ensure the promising features of TiN–NiMo reinforcements for Ni-based alloys. Produced coatings showed excellent performance under high-stress abrasion with wear values lower than for industrially used WC/W2C reinforced coatings.

I. INTRODUCTION

Coatings and surface treatments have proved to be a successful approach for increasing machinery lifespan by preventing severe wear and corrosion of working tools [1–3]. One of the attractive surface treatment methods is hardfacing by welding technique. This method offers the ability to apply thick protective coatings metallurgically bonded to the substrate material. Many hardfacing techniques such as laser cladding, gas-tungsten arc welding (GTAW), gas-metal arc welding (GMAW) and plasma transferred arc (PTA) are widely employed for deposition of a protective layer on a surface of a bulk material subjected to severe working conditions [4–6]. The most common coatings applied by hardfacing are metal matrix composites (MMCs) consisting of Ni, Co or Fe-based matrix, and reinforced with hard ceramic particles such as tungsten carbides

[5,7,8]. Tungsten carbide based hard metals are widely used in tribo-conditions because of their high abrasion and combined impact/abrasion wear resistance [9,10]. However, due to their poor oxidation resistance at elevated temperatures, WC-based composites are a less than ideal choice for tooling parts exposed to temperatures exceeding 550 °C [11]. Titanium Nitride (TiN) can be considered as an attractive reinforcement for MMCs because of its high hardness, quite low density, good oxidation resistance and high wear resistance in erosion and abrasion environments [12–15]. Several attempts have been made to apply titanium carbide powders by hardfacing using different processing methods. For the powder feeding method, TiN-based powder and metal matrix powder are delivered into the laser or plasma beam, melted and deposited onto the substrate [4,5,16]. This method enables a uniform distribution of primary hard phases in the matrix and results in low carbide dissolution. Alternative methods include mixing TiN and metal matrix, pre-placing the powder mixture on the surface of the substrate with the help of an organic binder and forming a coating layer to be clad [17,18]. The coatings deposited by these techniques are mostly characterised by formation of a gradient distribution of hard phase and are highly affected by dilution and its influence on the microstructure of the final product. A promising method for the reinforcement of metal matrix with TiN particles using laser cladding involves in-situ synthesis of TiN by reaction of titanium and graphite during laser processing [19,20]. Such hardfacings are characterised by excellent metallurgical bonding between the coating and the substrate and the high quality of the deposited material. However, because of TiN's low density, a uniform distribution of hard phases is not easily achieved. During solidification, the TiN particles show a gradient distribution in the matrix with respect to size and volume fraction [20]. Although titanium carbides are widely applied as reinforcements using different cladding technologies, there is a lack of information about processing of recycled TiN-based cermets as reinforcements for a nickel-based matrix with the PTA process. In the present study, titanium carbide reinforced hardfacings have been produced by the PTA technique using the powder feeding method. The precursor materials used were re-milled TiN-20% Ni:Mo (2:1) cermets added into the NiCrBSi matrix alloy. The coatings have been deposited onto an austenitic steel substrate. The main objectives of the work were: (i) to deposit NiCrBSi hardfacing coatings reinforced by TiN–NiMo cermet particles; (ii) to examine the microstructure and mechanical properties of the developed hardfacings; and (iii) to study the wear resistance of the coatings under three body abrasive wear conditions.

II. EXPERIMENTAL DETAILS

2.1. Powders

Pre-processed powder of titanium carbide based and nickel–molybdenum bonded cermet particles was used in the present study. These cermet particles were re-milled from the bulk of TiN-20 wt.% Ni:Mo (2:1) and then sieved to obtain the fraction 150...310 μm using collision milling method. To obtain cermet particles with the predetermined granulometry, multistage milling (up to 16 times) was used [21]. A representative SEM micrograph of the powder is shown in Fig. 1. NiCrBSi alloy powder (0.2% C, 4% Cr, 1% B, 2.5% Si, 2% Fe, rest Ni) with particle size of 50 ... 150 μm was used as a matrix material for the PTA process.

2.2. Plasma transferred arc hardfacing

PTA hardfacing of TiN–NiMo particles in combination with NiCrBSi matrix was carried out using a EuTronic® Gap 3001 DC apparatus. Austenitic stainless 1.4301 steel was used as a substrate. The coating thickness was set to 2.0–2.5 mm. The coating of the identical matrix alloy with the same volume

percentage of WC/W₂C reinforcements (Castolin Eutectic EuTroLoy PG 6503 alloy) was used as referencematerial for the wear testing.

2.2. Characterisation

Prior to testing, the samples were cut from large pieces, ground and subsequently polished using 1 μm diamond paste. A comprehensive microstructural evaluation of the plasma hardfacing was performed by optical microscopy (OM) with a digital camera (MEF4A, Leica Microsystem) and scanning electron microscopy (SEM Philips XL 30FEG), equipped with an energy dispersive X-ray analyser (EDX) with Dual BSD detector and operating at an accelerating voltage of 20 kV. For EDX quantification the standardless EDAX ZAF quantification method was used. The microstructural examination (OM) was conducted on the samples etched with a solution of HF and HNO₃ in volume ratio 1:12 at room temperature for 2 s. X-ray diffraction (XRD) experiments were performed on an X-Pert powder diffractometer (PANalytical, Netherlands) in continuous mode using CuK α radiation in Bragg–Brentano geometry at 40 kV and 30 mA. The diffractometer was equipped with a secondary graphite monochromator, automatic divergence slits and a scintillation counter. The hardness was determined by standard Vickers hardness testing at a load of 50 kgf (HV50). Average hardness values were calculated from 8 indents per specimen. The choice of such a high load was conditioned by the microstructural features of multiphase hardfacings, where under load of 10 kgf (10HV) a large scatter of hardness values for similar multiphase structures was obtained [22]. To evaluate the mechanical properties of constituent phases, nanoindentation measurements were performed using a Hysitron Triboindenter TI900 (Minneapolis, MN, USA) equipped with a diamond Berkovich indentation tip with 100 nm tip radius. The load cycle comprised loading for 5 s to reach the peak load of 10 mN and subsequent unloading for 5 s. The load vs. depth curves were analysed to determine the reduced elastic modulus and hardness using the procedure described elsewhere [23]. Nano-scratch testing was also performed with the Hysitron Triboindenter TI900 using the Berkovich tip as described above. The load during the scratches was set to a constant value of 5 mN. The length of all scratches was 20 μm with a scratch rate of 0.2 $\mu\text{m/s}$. 2.4. Wear testing The abrasive wear performance was evaluated using three-body abrasion tester by variation of testing conditions: a) use of a dry-sand rubber wheel according to ASTM G65 requirements; b) application of a steel wheel to simulate high-stress wear behaviour of materials. Rotation speed, normal load and sliding distance were kept constant at 200 rpm, 130 N and 4309 m, respectively. Ottawa silica sand with particle size of 212–300 μm was used as abrasive. Before and after testing each specimen was cleaned with acetone, dried and weighed. At least three tests were run for each material to determine the wear resistance.

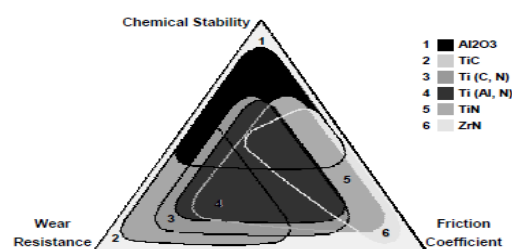


Figure 8: The Main Properties of Various Coating Layers.

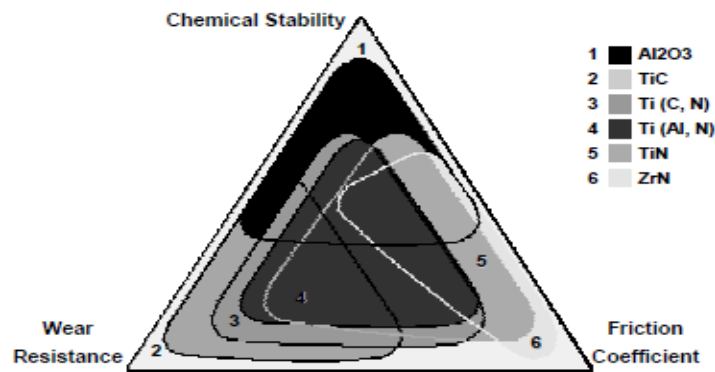


Figure 8: The Main Properties of Various Coating Layers.

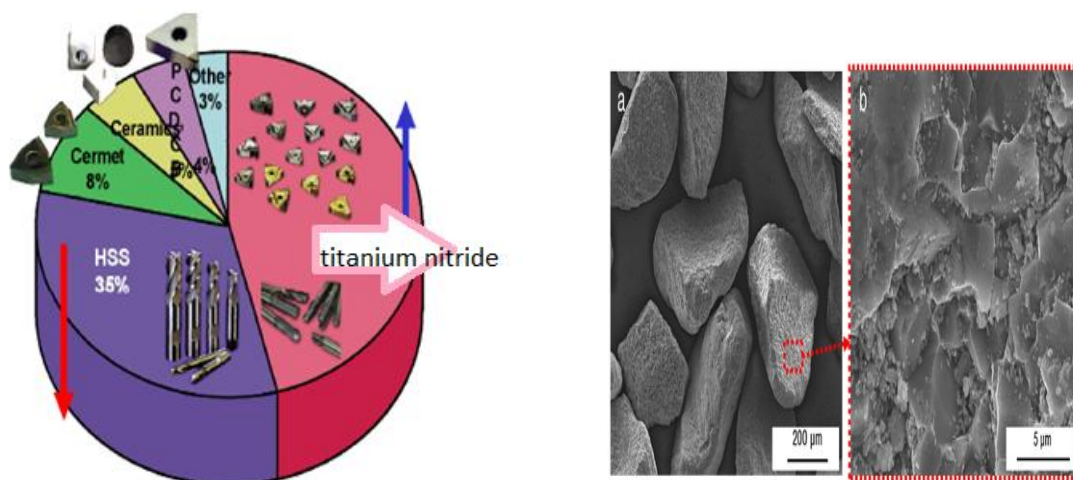


Fig. 1. SEM images of TiC-NiMo particles: (a) overview; (b) surface of the particle.

III. RESULTS AND DISCUSSION

3.1. Deposition

Deposits of the TiN–NiMo and NiCrBSi alloy powders in the ratio of 40:60 vol.% were processed onto an austenitic stainless steel substrate. The selection of proportion for PTA hardfacings can be attributed to the low density of TiN-based reinforcements, where 40 vol.% of hard phases was suggested to be optimal for uniform hard particles distribution [24]. Two separately controlled powder feeders were used for the adjustment of the required powder ratio. The powders were transported internally through the welding torch with the help of a carrier gas and then introduced into a molten weld pool which after solidification formed a metallurgically bonded layer on the surface of the base metal as schematically shown in Fig. 2. Optimised hardfacing process parameters are listed in Table 1. The parameters of deposition of TiN–NiMo phase are influenced by certain porosity; high welding energy (welding current up to 100 A and high plasma gas flow rate) is required to overcome this problem and minimize porosity level in a welding seam. Due to low density of TiN–NiMo reinforcements (~5.5 g/cm³), which is significantly lower than density of nickel-based alloy (~8.5 g/cm³), cermet particles float upward in the molten pool during solidification and almost no cermet particles remain at the close proximity to a coating base. The high carrier gas flow and pressure rates were found to improve the distribution of hard particles during deposition. Fig. 3 illustrates the TiN–NiMo reinforced NiCrBSi weld overlay. The OM examination reveals a uniform distribution of hard phases in the matrix, negligible porosity of

www.ijarse.com

the hardfaced layer and overall good quality of the welding seam with minimal dilution with the substrate of less than 5% according to the quantitative analysis. The obtained coating seems to be metallurgically well bonded to the austenite substrate.

3.2. Microstructural analysis

Fig. 4 illustrates the microstructure of the cermet particle reinforced hardfacing. The following apparent phases were detected: dendritic Ni-based matrix, TiN-based precipitates of less than 2 μm in diameter, and TiN–NiMo cermet grains. Both hard phases were homogeneously distributed throughout the matrix. The nickel binder in the cermet particle is assumed to protect the primary carbides from dissolution. The XRD pattern of TiN–NiMo reinforced NiCrBSi hardfacing is presented in Fig. 5.

The analysis reveals five crystalline phases:

Ni-rich dendritic matrix — $\gamma(\text{Fe,Ni})$; $(\text{Fe, Ni, Mo})_2\text{3B}_6$, which is the most probable Fe–Ni–B hard phase located in dendrites with some traces of Mo in the crystal lattice; TiC phase; non-stoichiometric carbide $\text{Ti}_{0.92}\text{Mo}_{0.02}\text{N}_{0.6}$; and $(\text{Mo, Ti})\text{N}$. Formation of solid solutions of Mo in the TiN lattice results in development of so-called core-rim structured grains consisting of a TiN core surrounded by the rim of $(\text{Ti,Mo})\text{C}$ [25–27]. Fig. 6 presents SEM micrographs of the TiN–NiMo reinforced hardfacing. The PTA welding process does not significantly influence the structure and composition of the cermet particles. However, it is found that besides a high amount of TiN-based spherical precipitates (Fig. 6d), TiN diffusing from the cermet zone to the matrix during deposition the structure of cermet particles along the interface (Fig. 6b) differs from the microstructure of the cermet particles at the core (Fig. 6c). The particles near the interface are partially dissolved showing decrease in grain size and modification in their shape. However, partially dissolved grains are still core-rim structured TiN– $(\text{Ti,Mo})\text{N}$ particles as confirmed by the EDX analysis of spots 1 and 2 indicated in Fig. 6b and c and shown in Table 2. Table 2 identifies the chemical composition (wt. %) of TiN–NiMo reinforced hardfacing examined with energy dispersive X-ray (EDX) analysis. Results presented in Table 2 show average values of at least 5 spot analyses. The corresponding EDX spots are labelled with numbers in Fig. 6. Spot 1 corresponds to the core part of the TiC based grain and shows only Ti and C, i.e. a TiC phase. Spot 2 was of Mo with a concentration varying between 4 and 12 wt.%. This distribution of elements, verified at approximately 5 spots taken at the rim part, confirms the presence of the $(\text{Ti,Mo})\text{N}$ phase, which according to the XRD results can be non-stoichiometric carbide.

3.3. Mechanical properties

3.3.1. Hardness

The measured Vickers hardness of the pure NiCrBSi matrix was $365 \pm 15 \text{ HV}_{50}$, which is in good agreement with the previous study [22]. The macro hardness of the TiN–NiMo reinforced hardfacing is $571 \pm 25 \text{ HV}_{50}$. The hardness increase is probably due to the high content of uniformly distributed cermet particles and TiC-based precipitations.

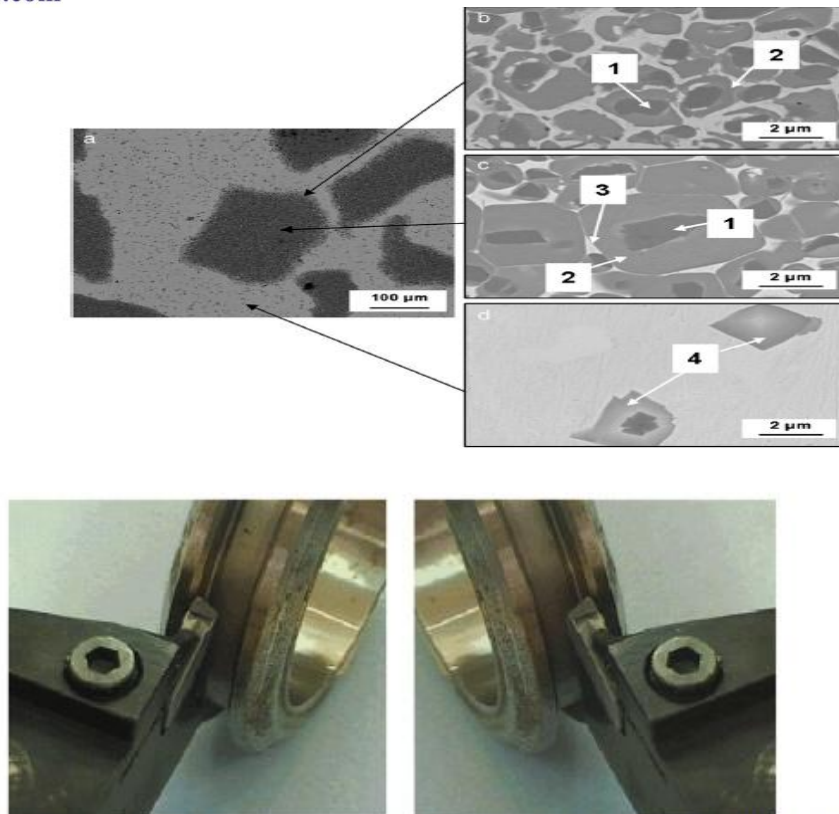


Figure 16: Machining a Synchronizing Ring with CBN CUT-GRIP Tools.

General Operating Characteristics of Cutting-tool Materials

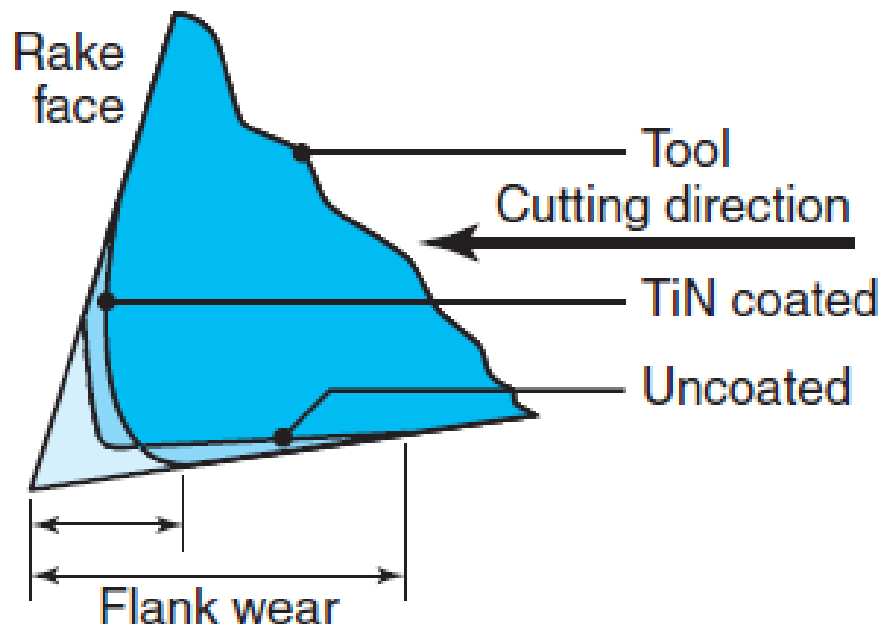
Tool materials	General characteristics	Modes of tool wear or failure	Limitations
High-speed steels	High toughness, resistance to fracture, wide range of roughing and finishing cuts, good for interrupted cuts	Flank wear, crater wear	Low hot hardness, limited hardenability, and limited wear resistance
Uncoated carbides	High hardness over a wide range of temperatures, toughness, wear resistance, versatile, wide range of applications	Flank wear, crater wear	Cannot use at low speeds because of cold welding of chips and microchipping
Coated carbides	Improved wear resistance over uncoated carbides, better frictional and thermal properties	Flank wear, crater wear	Cannot use at low speeds because of cold welding of chips and microchipping
Ceramics	High hardness at elevated temperatures, high abrasive wear resistance	Depth-of-cut line notching, microchipping, gross fracture	Low strength and low thermomechanical fatigue strength
Polycrystalline cubic boron nitride (cBN)	High hot hardness, toughness, cutting-edge strength	Depth-of-cut line notching, chipping, oxidation, graphitization	Low strength, and low chemical stability at higher temperature
Diamond	High hardness and toughness, abrasive wear resistance	Chipping, oxidation, graphitization	Low strength, and low chemical stability at higher temperatures

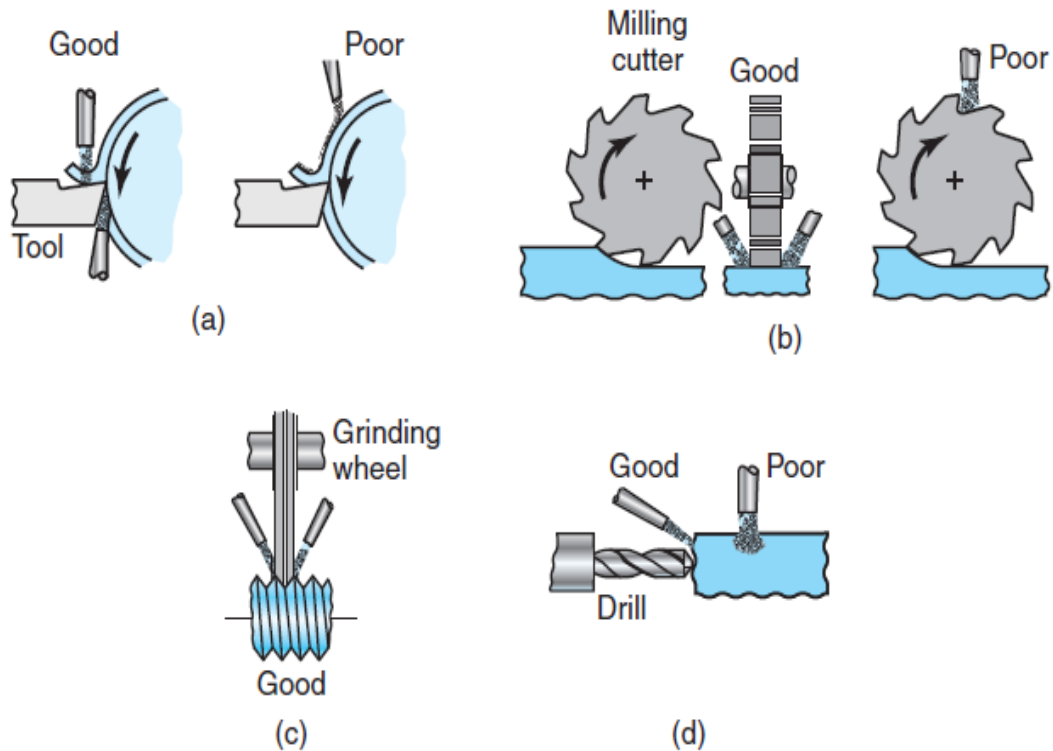
Source: After R. Komanduri and other sources.

General Operating Characteristics of Cutting-tool Materials

Tool materials	General characteristics	Modes of tool wear or failure	Limitations
High-speed steels	High toughness, resistance to fracture, wide range of roughing and finishing cuts, good for interrupted cuts	Flank wear, crater wear	Low hot hardness, limited hardenability, and limited wear resistance
Uncoated carbides	High hardness over a wide range of temperatures, toughness, wear resistance, versatile, wide range of applications	Flank wear, crater wear	Cannot use at low speeds because of cold welding of chips and microchipping
Coated carbides	Improved wear resistance over uncoated carbides, better frictional and thermal properties	Flank wear, crater wear	Cannot use at low speeds because of cold welding of chips and microchipping
Ceramics	High hardness at elevated temperatures, high abrasive wear resistance	Depth-of-cut line notching, microchipping, gross fracture	Low strength and low thermomechanical fatigue strength
Polycrystalline cubic boron nitride (cBN)	High hot hardness, toughness, cutting-edge strength	Depth-of-cut line notching, chipping, oxidation, graphitization	Low strength, and low chemical stability at higher temperature
Diamond	High hardness and toughness, abrasive wear resistance	Chipping, oxidation, graphitization	Low strength, and low chemical stability at higher temperatures

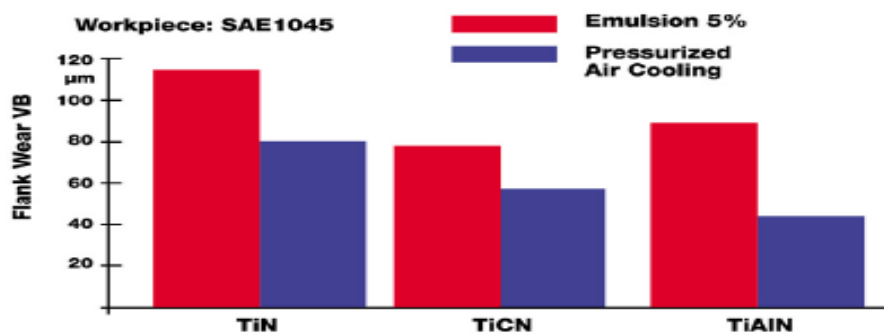
Source: After R. Komanduri and other sources.





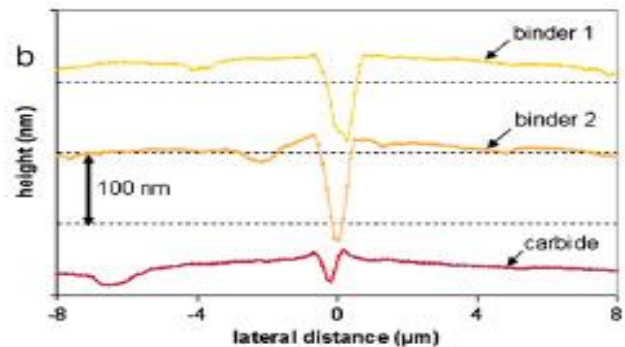
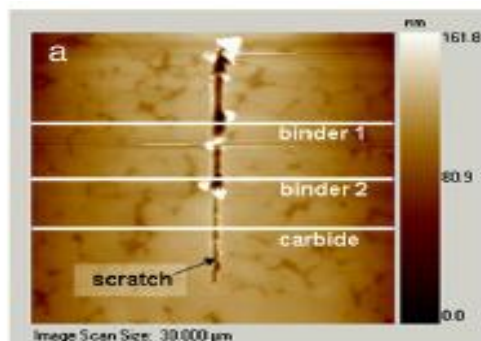
3.5. Abrasive wear behaviour

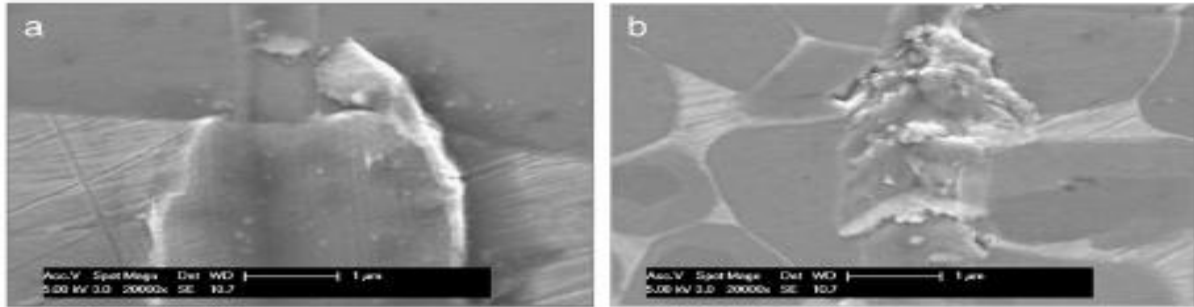
Wear tests exploiting steel and rubber wheels were carried out to reproduce three-body abrasion process. Quantitative wear analysis was performed by determination of volume loss, Fig. 12. The relative wear resistance of the TiN–NiMo reinforced hardfacing was compared to conventionally used Ni-based reference hardfacing consisting of 40 vol.% of WC/W₂C particles (Castolin Eutectic EuTroLoy PG 6503 alloy). Generally, both materials under investigation indicate low wear values; however, conventionally used tungsten carbide reinforced coating shows approximately 40% higher wear resistance. The volumetric wear values of the materials tested with steel wheel are drawn on the abscissa. Wear of the commercially used WC/W₂C reinforced alloy is significantly increased (almost by a factor Fig. 8. Calculated modulus of elasticity (E) vs. hardness (H) of different phases in the TiC–NiMo reinforced NiCrBSi hardfacing measured by nanoindentation. Fig.



Designation	Workpiece Material	Carbide Grade	Vc (m/min)	fz mm/z	Tool Life TL
SEKR 1203 AFN-76	17-4 PH	IC 328	120	0.1	30'
SEKR 1203 AFN-42					20'
SEKR 1203 AFN-76	17-4 PH	IC 328	80	0.1	50'
SEKR 1203 AFN-76	Inconel	IC 328	25	0.1	28'
SEKR 1203 AFN-42					18'

of three), while wear of TiN–NiMo reinforced coating remains at almost the same low level. It is well known that abrasive wear behaviour is strongly influenced by material hardness and microstructural features [33]. Under conditions of three-body abrasion several wear mechanisms can dominate depending on material of a testing wheel. Exploitation of a rubber wheel simulates low stress abrasion, while application of a steel wheel results in a high stress mode of abrasion characterised by other mechanisms of material removal as compared to mechanisms operating at low stress wear mode. To study the wear mechanisms, SEM surface sectional images of the worn areas were examined as shown in Fig. 13. High performance of WC/W₂C reinforced alloy under testing with a rubber wheel is in a good correlation with previous studies [6,7], where the high matrix hardness and dense distribution of coarse primary carbides ensure excellent wear resistance (Fig. 13a). Moreover, the secondary precipitations in matrix do not negatively influence the low-stress abrasion resistance and no cracks were detected by scanning electron microscopy. For the TiC–NiMo reinforced alloy the increase in wear rate can be attributed to low hardness of the matrix material. The titanium Nitride based precipitates are small enough for successful protection of the matrix against coarse silica abrasive particles (Fig. 13c). The dominant wear mechanisms in this case are ploughing and cutting of ductile Ni-based matrix. Additionally, the inter-particle distances between cermet reinforcements are large that leads to the formation of hills in cermet supported areas of the matrix. The behaviour of a material in a rotating wheel abrasion test depends not only on the intrinsic properties of the test piece itself, but also on the conditions of the test [34]. Application of a steel wheel can cause a significant fragmentation of abrasive particles or their embedment into the surface of base material [35]. Certain ductility





and specific microstructural arrangement are required to increase the abrasive wear resistance of multiphase materials. For the WC/W₂C reinforced hardfacing (Fig. 13b) the brittle fracture of both primary carbides and matrix precipitates was observed; extensive cracking and subsequent chip removal explain a significant increase in wear rate by a factor of three. Compared to the brittle fracture behaviour of the Ni-based reference hardfacing consisting of 40 vol.% of WC/W₂C particles, the TiN–NiMo reinforced alloy performs in a more ductile way (Fig. 13d), where no well pronounced brittle fracture of hard particles was detected: neither matrix precipitates nor cermet particles indicate extensive crack formation. These results can be also correlated with the data obtained during nano-scratching, where no cracking of hard particles was detected.

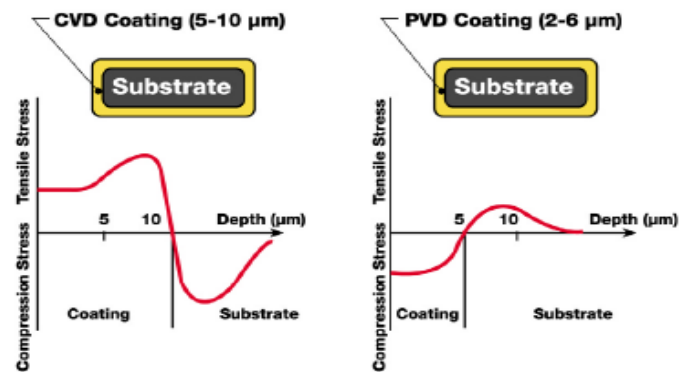


Figure 10: Stress Distribution in PVD and CVD Coated Layers.

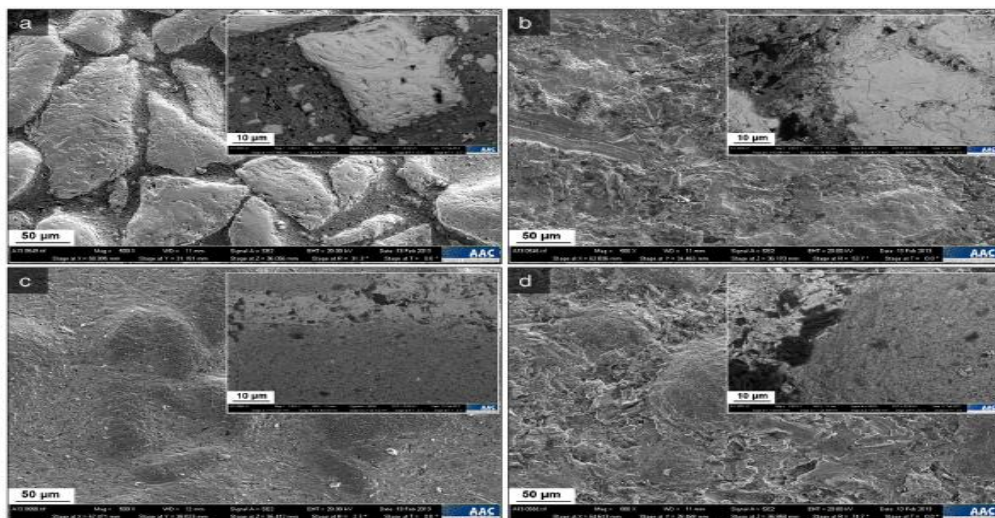


Fig. 13. SEM micrographs of worn hardfacing surfaces after three-body abrasion tests: a) and b) WC/W₂C reinforced coating – rubber and steel wheel; c) and d) TiC–NiMo reinforced coating – rubber and steel wheel.

Based on the study within this work, the following conclusions can be drawn:

- The titanium carbide based cermet particles recycled from TiNMo₂C-Ni composites' scrap and applied for hardfacings deposition using the PTA technology can be successfully used for deposition of thick coatings characterised by uniform distribution of constituents and low level porosity.
- The mechanical properties of the TiN and (Ti,Mo)Ni phases measured by nanoindentation are very similar exhibiting a narrow distribution of the hardness and Young's modulus values. Both carbide and precipitate phases indicate similar high hardness values, whereas the precipitate phase has significantly lower Young's modulus.
- The nano-scratching test reveals excellent bonding between the matrix and cermets in the hardfacing. No extensive cracking was detected in the interface matrix/hard phase region.
- The performance of the TiN-NiMo reinforced hardfacings under low stress three-body abrasion is lower as compared to the commercially used WC/W₂C reinforced coatings. Wear mechanisms operating in TiN-NiMo reinforced alloy are matrix material ploughing and cutting. Fine structured TiN-based precipitates do not provide sufficient protection against coarse abrasive particles.
- Under high-stress three-body abrasion TiN-NiMo reinforced hardfacings show significantly higher wear resistance as compared to commercially used WC/W₂C reinforced coatings. The tungsten carbide reinforced coating shows brittle fracture of the coarse primary carbides and secondary precipitates, while fine-grained structure of TiN-NiMo reinforcements is not subjected to extensive cracking during the test.

V. ACKNOWLEDGEMENTS

This work was funded by the "Austrian Comet-Program" (governmental funding program for pre-competitive research) via the Austrian Research Promotion Agency (FFG) and the TecNet Capital GmbH (Province of Niederösterreich) and has been carried out within the "Austrian Center of Competence for Tribology" (AC2T research GmbH) in cooperation with Tallinn University of Technology and Vienna University of Technology. Part of this work was supported with EFRE funding and with support of the country of Lower Austria within the project "Onlab". This work has been also partially supported by graduate school "Functional SEM images, materials and technologies", receiving funding from the European Social Fund under project 1.2.0401.09-0079 in Estonia. The authors would like to acknowledge Estonian Science Foundation under grant ETF 8211 for the support of the study. The authors are also grateful to Dmitrij Goljandin, MSc, and Der-Liang Yung, MSc, from Tallinn University of Technology for their contribution into research and to Dr. Christian Jogl from AAC (Aerospace & Advanced Composites GmbH) for the support with SEM images .

REFERENCES

- [1] B.G. Mellor, Surface Coatings for Protection Against Wear, Chapter 9, Woodhead Publishing Limited, Cambridge, 2006, p. 302.
- [2] R. Chattopadhyay, Kluwer Academic Publishers, New York, 2004, p. 1.
- [3] E. Badisch, C. Katsich, H. Winkelmann, F. Franek, M. Roy, Tribol. Int. 43 (2010) 1234.
- [4] R.L. Deuis, J.M. Yellup, C. Subramanian, Compos. Sci. Technol. 58 (1998) 299.
- [5] J. Nurminen, J. Nötkki, P. Vuoristo, Int. J. Refract. Met. Hard Mater 27 (2009) 472.

www.ijarse.com

- [6] M. Kirchgaßner, E. Badisch, F. Franek, *Wear* 265 (2008) 772.
- [7] C. Katsich, E. Badisch, *Surf. Coat. Technol.* 206 (2011) 1062.
- [8] S. Chatterjee, T.K. Pal, *Wear* 261 (2006) 1069.
- [9] S. Ndlovu, *The Wear Properties of Tungsten Carbide-Cobalt Hardmetals from the nanoscale up to the Macroscopic Scale*, PhD thesis, Erlangen, 2009.
- [10] I. Hussainova, *Wear* 258 (2005) 357.
- [11] J. Kuzmanovic, *WC-W2C Particle Reinforced Powder Metallurgy Iron and Nickel Matrix Composites Produced by Pressing and Sintering*, MSc thesis, Vienna TU, 2011.
- [12] S. Cardinal, A. Malchere, V. Garnier, G. Fantozzi, *Int. J. Refract. Met. Hard Mater* 27 (2009) 521.
- [13] I. Hussainova, *Wear* 255 (2003) 121.
- [14] J. Kübarsepp, H. Klaasen, J. Pirso, *Wear* 249 (2001) 229.
- [15] M. Antonov, I. Hussainova, *Tribol. Int.* (2009) 1566.
- [16] Y.P. Kathuria, *Surf. Coat. Technol.* 140 (2001) 195.
- [17] R.L. Sun, Y.W. Lei, W. Niu, *Surf. Coat. Technol.* 203 (2009) 1395.
- [18] S. Yang, M. Zhong, W. Liu, *Mater. Sci. Eng. A* 343 (2003) 57.
- [19] X.H. Wang, S.L. Song, Z.D. Zou, S.Y. Qu, *Mater. Sci. Eng. A* 441 (2006) 60.
- [20] S. Yang, N. Chen, W. Liu, M. Zhong, Z. Wang, H. Kokawa, *Surf. Coat. Technol.* 183 (2004) 254.
- [21] P. Kulu, S. Zimakov, *Surf. Coat. Technol.* 130 (2000) 46.
- [22] A. Zikin, I. Hussainova, C. Katsich, E. Badisch, C. Tomastik, *Surf. Coat. Technol.* 206 (2012) 4270.
- [23] G.M. Pharr, W.C. Oliver, F.R. Brotzen, *J. Mater. Res.* 7 (1992) 613.
- [24] A. Zikin, S. Ilo, P. Kulu, I. Hussainova, C. Katsich, E. Badisch, *Mater. Sci. Medžiagotyra* 18 (2012) 12.
- [25] Y.K. Kim, J.H. Shim, Y.W. Cho, H.S. Yang, J.K. Park, *Int. J. Refract. Met. Hard Mater* 22 (2004) 193.
- [26] I. Hussainova, A. Kolesnikova, M. Hussainov, A. Romanov, *Wear* 267 (2009) 177.
- [27] Z. Liu, L. Zhao, Y. Bao, B. Li, *Adv. Mater. Res.* 194–196 (2011) 1785.
- [28] A.O. Kunrath, I.E. Reimanis, J.J. Moore, *J. Alloys Compd.* 329 (2001) 131.
- [29] I. Hussainova, E. Hamed, I. Jasiuk, *Mech. Compos. Mater.* 46 (2011) 667.
- [30] F. Sergejev, E. Kummari, M. Viljus, *Procedia Eng.* 10 (2011) 2873.
- [31] H. Berns, *Wear* 181–183 (1995) 271.
- [32] M.G. Gee, A. Gant, B. Roebuck, *Wear* 263 (2007) 137.
- [33] H. Winkelmann, E. Badisch, M. Kirchgaßner, H. Danninger, *Tribol. Lett.* 34 (2009) 155.
- [34] S. Wirojanupatump, P.H. Shipway, *Wear* 239 (2000) 91.
- [35] M. Antonov, I. Hussainova, R. Veinthal, J. Pirso, *Tribol. Int.* 46 (2012) 261.



Associate Professor with HOD & Research scholar in -VTU, Department of Mechanical Engineering, Newtons institute of science and technology College, Guntur, AP, India